THE STEADY STATE FLOW OF THE MODIFIED REINJECTION SYSTEM OF THE BACMAN 1 GEOTHERMAL PRODUCTION FIELD, PHILIPPINES

R C. Bobis

PNOC Energy Development Corporation, Merritt Road, Ft. Bonifacio, 1201 Makati City, Philippines

ABSTRACT

The Bacman 1 Reinjection system was designed to conduct hot brine in rugged terrain over a 62-meter hump. Automatic pressure control valves maintained pressure upstream of this hump above fluid saturation thus preventing large pressure transients associated with column separation and rejoining. When these valves were removed the system's tolerance for pressure and flow fluctuations have to be assessed to design appropriate operating procedures for the modified system.

The aim of this project is to create a steady state flow model of the modified Bacman 1 reinjection system that will allow pressure transient simulator softwares to evaluate system's response to flow and pressure fluctuations. It is also designed to assess how the steady state flow model varied with changes in mass flows, heat transfer and pipe friction losses. These will provide information for selection of an optimum reinjection utilization strategy.

The model that was conceived had two-phase flow occurring as much as 10 meters below the hump on its upstream side. Variations in the stable water level of the liquid column upstream of the hump, when the mass flow, friction loss and heat loss rate changed, were minimal to influence the reinjection line utilization strategy. A pressure transient simulation with appropriate software is still recommended to confirm these results.

1.0 INTRODUCTION

The 110 MWe Bacman 1 Geothermal Production Field is located in a mountainous region near the southern tip of Luzon 550 kilometers south of Manila. All the hot brine separated from the two-phase fluid is reinjected by gravity through reinjection wells. Due to the considerable cost it would take to level the area, the Reinjection (RI) system was designed with a 120-m drop in elevation and a 62-m hump in the middle of the 3.6 km pipeline. It included automatic pressure control valves that smooth out small pressure and flow fluctuations that could trigger large pressure transients. These valves prevented the flashing of the RI fluids during large pressure fluctuations by pressurizing the upstream pipe section above the flash point. At the start of commercial operation in September 1993, the Hump Station control valves were operated as designed. System over pressure associated with the valves' automatic operation however caused bursting discs to rupture often. Silica deposits caused the valves to stick and actuate in jerky motion that resulted in high-pressure transients upstream. These valves were then operated at full open conditions for two years during which no pressure transients were experienced. In 1997 these control valves were removed altogether. As a consequence it is possible that the RI system has lost tolerance for pressure and flow fluctuations. Large pressure transients are more likely to be triggered by smaller pressure and flow fluctuations than when the valves were still in place. This can be assessed with computer pressure transient simulations provided that a steady state flow model of the whole RI pipeline has been set up. Another important point to assess is how changes in mass flow, pipe heat loss during weather swings and pipe friction loss affect the stability of the steady state flow model.

The Bacman 1 reinjection system (Fig. 1) allows hot water from two different separator stations to be fed into the reinjection line of either station at three interconnection points. It also allows utilization of four wells at three different well pads. From the six separator vessels at Separator Station 1 (SS1), 250-mm lines go into a 600-mm header. This main RI header descends into Pad C where it comes along side an identical RI line from four separator vessels at Separator Station 2 (SS2). At Pad C the first interconnection of the two lines is located at an elevation of 598 m. The lines then dip into the Low Point Station (LPS) where part of the hot water from each is diverted to a

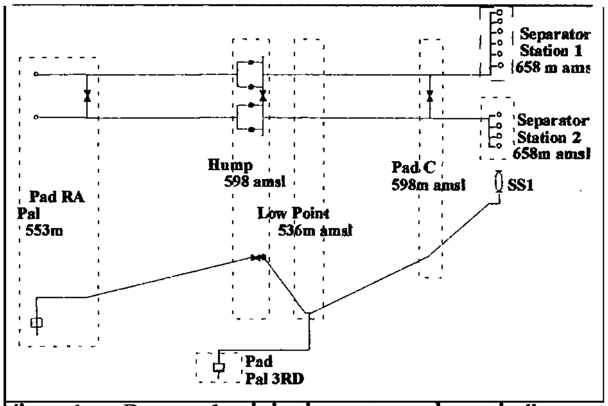

'igure 1. Bacman 1 **reinjection system schematic diagran and elevation profile.**

450-mm line to well Pal-3RD at Pad RC/RD. From the LPS the bulk **of** the fluid continue upwards to the Hump Station (HS) where the lines enter a 760 mm header. This acts as the second interconnection between the two main RI lines. From this, **four 400**-mm lines each containing a **300-mm** pneumatically actuated butterfly valve (Fig. 1) slope downward. Downstream the **four** lines join back to two 600 mm-lines which continue on to Pal 1. Further downhill the lines terminate into Pal **1RD** and **4RD** at **RI** Pad RA where the third interconnection is located.

Based on a simplified line diagram **of** one 600-mm RI line and the pressures measured at certain pipe locations, the hydraulic gradient lines (HGL) at **three** different flow-situations were deduced. From these, the steady state flow model for the RI system was conceived in terms of flow regimes and pipeline water levels. To predict the changes on this model as the pipe friction loss varied, zero heat loss was assumed in the analysis of the simplified Bernoulli equation. This then led to assumptions used in assessing the changes on the flow model as the mass flow varied. To assess the effects of heat loss due to weather swings, two different weather conditions were assumed and applied on the **three** flow situations.

2.0 THEORIES AND EQUATIONS

The following equations, theories and principles were used in this study:

$$\text{HGL} = \frac{P}{\quad} + Z \qquad (1)$$

The Hydraulic Gradient Line, HGL, is defined as the sum **of** the pressure head and the elevation head. It represents the mechanical energy level **of** a fluid at a point if the velocity head is neglected. It is helpful in analysis **of** fluid flow involving fictional losses. In open channel flow the HGL is identical to the **free** surface **of** the water when the pressure head is neglected (White).

$$\frac{h_1}{g} + Z_1 = \frac{h_2}{g} + Z_2 + \frac{h_{q(1-2)}}{g} \qquad (2)$$

The simplified Steady Flow Energy Equation (SFEE) above was used to calculate the specific-enthalpy **of** the RI fluid and thus determine the fluid state at the defined points.

$$\frac{P_1}{\rho_1 g} + Z_1 = \frac{P_2}{\rho_2 g} + Z_2 + h_f \qquad (3)$$

The Bernoulli equation above with the velocity head neglected was used to calculate the water level elevations and pressure at points in the RI line.

$$h_f = \frac{\lambda L V^2}{D 2g} \qquad (4)$$

$$h_f = \frac{\lambda L V^2}{D_H 2g} \qquad \text{where: } D_H = 4R_H \qquad (5)$$

The Darcy-Weisbach equations above were used **for** the calculation **of** pipe fiiction **loss** for full pipe flow and partially filled pipe flow **(uniform** open channel flow).

$$Q/L = \frac{2\pi\Delta T}{\frac{1}{h_i r_i} + \frac{\ln(r_2/r_1)}{k_s} + \frac{\ln(r_3/r_2)}{k_p} + \frac{\ln(r_4/r_3)}{k_{fg}} + \frac{1}{h_o r_4}} \qquad (6)$$

For full pipe flow the heat loss per pipe unit length, Q/L, was calculated with the Heat Flow Through Insulated Pipe Equation above.

3.0 METHODOLOGY

The following steps were taken to achieve the study objectives:

1) A simplified line diagram (Fig. 2) of the 600-mm RI line fiom SSI to RI Pad RA was drawn with five sections bordered by six points P1, P2, P3, P4, P5 and P6. The sections are referred to with its termination points such as Section 1-2 for the pipe section between points P1 and P2.

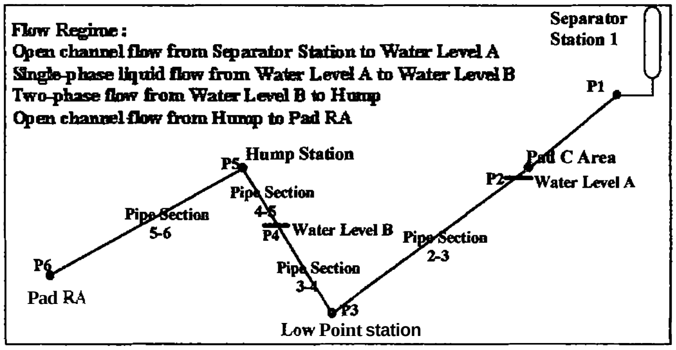

Figure 2. Simplified line diagram and sectioning showing the flow regime per section

2) The Hydraulic Gradient Lines (HGL) of the simplified line diagram were drawn based on actual pressure measurements at P1, P3; P5 and P6 during three RI flow situations namely:
   a) Situation 7, S7 (Fig. 3). The flow fiom SS2 **at slightly lower pressure and temperature mixes with the flow from SS1 iust upstream of P2. The** RI well Pal 3RD is "out of service thus the flow fiom P2 to Low Point, P3, is equal to the flow from low point to the hump, P5.
   b) Situation 8, S8 (Fig. 4). The flow fiom SS2 does not mix with that from SS1, however, Pal 3RD is in service thus the flow in pipe section 3-4 is less than the flow in pipe section 2-3 by 65 kg/s.
   c) Situation 9, S9, (Figure 5). One 600-mm RI line with Pal 3RD is in service. All the flow fiom SS2 mixes with that fiom SS1 making the flow in pipe section 3-4 less than those in pipe section 2-3 by 130 kg/s. The separator stations in this situation operate at lower pressures than normal.

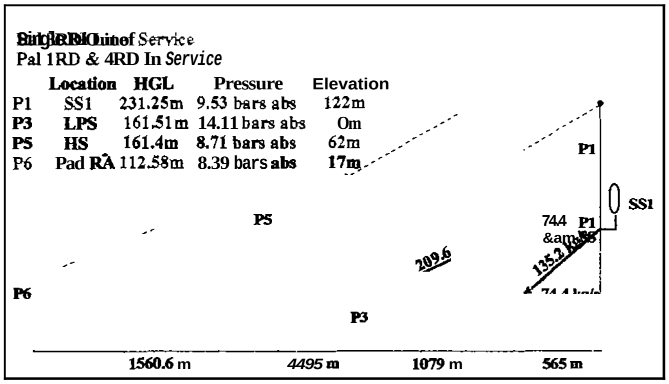

	Location	HGL	Pressure	Elevation
P1	SS1	231.25m	9.53 bars abs	122m
P3	LPS	161.51m	14.11 bars abs	0m
P5	HS	161.4m	8.71 bars abs	62m
P6	Pad RA	112.58m	8.39 bars abs	17m

Figure 3. **HGL of Situation 7.**

3) The flow regimes at different sections of the pipeline were determined by HGL analysis.

4) P_2, P_4 and the pipeline water levels were determined using the Bernoulli and the Darcy-Weisbach equations as applied to every two adjacent points. Zero heat loss in the pipelines and uniform open channel flow at section 1-2 were assumed.

5) The simplified Bernoulli equation was analyzed to determine the possible effects of the changes in pipe fiction loss brought by changes in the mass flow and pipe friction factor. In the process the assumption in creating hypothetical flow situations at different mass flows was arrived at.

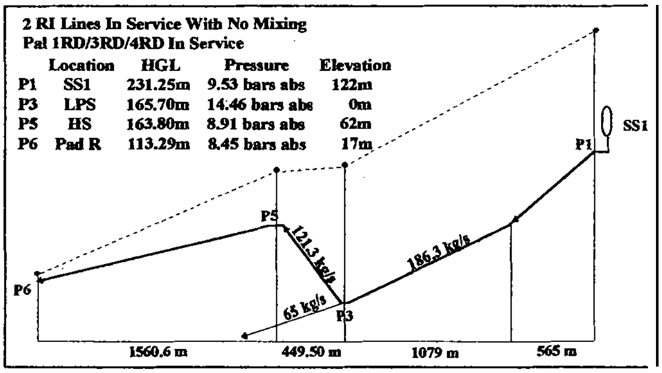

	Location	HGL	Pressure	Elevation
P1	SS1	231.25m	9.53 bars abs	122m
P3	LPS	165.70m	14.46 bars abs	0m
P5	HS	163.80m	8.91 bars abs	62m
P6	Pad R	113.29m	8.45 bars abs	17m

Figure 4. HGL of Situation 8.

6) To create flow situations with different heat loss rates, two weather conditions of different wind velocity and ambient temperature were assumed and applied to S7, S8 and S9. The state properties at different points and the line water levels were then determined by using the Bernoulli equation, the SFEE and the heat flow through insulated wall equation. These were then compared to each other to assess the possible effects of changes in heat loss rates to the Steady State Flow Model.

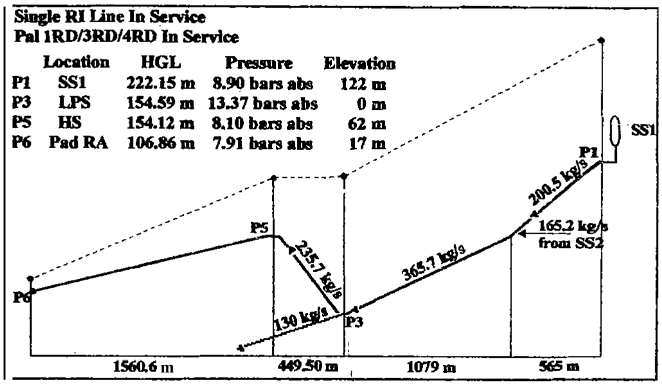

Figure **5**. HGL of **Situation 9.**

7) Based on S7 under the two assumed weather conditions, hypothetical flow situations were set up at two different mass flows to assess the changes these will bring to the Steady State Flow Model. Due to the number of variables involved, it was assumed that the changes in mass flow will bring changes only to P_3 and water level A. The changes in these two variables were then calculated using the same equations as in the previous step.

4.0 RESULTS AND DISCUSSION

4.1 Flow Regimes at Different Pipe Sections Determined by HGL Analysis

a) Separator Station to Pad C (Pipe section 1-2) - open channel flow
b) Pad C to Low Point (Pipe section 2-3) - **full** pipe liquid flow
c) Low Point to Flashing Point (Pipe section 3-4) - full pipe liquid flow
d) Flashing Point to Hump Station (Pipe section **4-5)** - two phase flow
e) Hump Station to Pad RA RI Wells (Pipe section ***5-6)*** - open channel flow

4.2 Discussion of the Results of the Pressure and Water Level Calculation with Assumed Zero Heat Loss

Table 1. Pressures and water levels with heat loss assumed equal to zero.

Situation	P_1	P_2*	P_3	P_4*	P_5	P_6	Water Level		ΔWL	Mass flow
							A	B		
	(bars)	(bars)	(bars)	(bars)	(bars)	(bars)	(m)	(m)	(m)	(kg/s)
S7	9.53	9.34	14.11	9.34	8.71	8.39	55.56	54.23	1.34	209.6/209.6
S8	9.53	9.53	14.46	9.53	8.91	8.45	57.28	56.37	0.91	186.3/121.3
S9	8.9	8.79	13.37	8.79	8.1	7.91	55.13	51.82	3.31	365.7/235.7

1) The results of the calculation in S9 show that the elevation at which the saturation pressure is reached can be as low as **10** meters below the hump elevation of 62 meters thus confirming that two phase flow occurs between P4 and the hump when heat loss is neglected.

2) $$\frac{P_3 - P_4}{\rho g} + (Z_3 - Z_4) = h_{f3-4}$$

An increase in the right hand side of the Bernoulli equation above when applied to section 3-4, has to be offset by an increase in either the pressure at the low point, P_3, a drop in Z_4, or both (the quantity Z_3-Z_4 is negative). A decrease in Z_4 is unlikely though because a higher friction loss will also be true in the two-phase flow at pipe section 4-5. This will naturally cause the water level to rise to cope with the higher flow resistance. It would then be safer to think that when heat loss is assumed at zero, Z_4 will remain the ***same*** at increased mass flow or friction factor. The pressure at the low point, P_3, will then have to increase.

The same simplified equation when rearranged to apply to pipe section 2-3 is

$$P_2 - P3 + \frac{(Z_2 - Z_3)}{\rho g} = hf2\text{-}3$$

If the friction loss, h_6 m section 2-3 increases due to an increase in either mass flow or fiction factor, two quantities *can* vary to compensate for *this*. P_3 has to decrease, Z_2 has to increase, *or* both. Since P_3 has to increase as determined in the similar analysis of section 3-4, Z_2 will have to increase. In effect water level A has to back up to overcome the additional pressure drop in section 2-3 as well as in section 3-4.

4 3 Results and Discussion of Water Level and Pressure Calculation with Heat Loss Considered

1) Table 2 shows increasing trend in both water levels A and B as heat loss increases from zero at Situation Sn to maximum at Situation Sn (21/10). This is due to the decrease in P_2 and P_4 associated with lower boiling temperatures bemuse of heat lost in the pipeline.

2) The difference in water levels A and B (AWL) representing the fiction loss in the pipelines, is effectively masked by the heat loss effect shown in its decreasing trend as heat loss increases. In fact water level B *can* at times be higher than water level A shown in Situation 8 in Table 2. This is probably because heat loss per unit mass of fluid is larger at lower fluid velocities and mass flows.

Table 2. Comparison of pressures and water levels with increasing heat loss.

Situation	P_1	P_2*	P_3	P_4*	P_5	P_6	Water Level		ΔWL	Mass flow
							A	B		
	(bars)	(bars)	(bars)	(bars)	(bars)	(bars)	(m)	(m)	(m)	(kg/s)
S7	9.53	9.34	14.11	9.34	8.71	8.39	55.56	54.23	1.34	209.6/209.6
S7(29/1)	9.53	9.3	14.11	9.20	8.71	8.39	56.00	55.78	0.22	209.6/209.6
S7(21/10)	9.53	9.28	14.11	9.17	8.71	8.39	56.23	56.11	0.12	209.6/209.6
S8	9.53	9.53	14.46	9.53	8.91	8.45	57.28	56.37	0.91	186.3/121.3
S8(29/1)	9.58	9.52	14.46	9.40	8.91	8.45	57.38	57.82	-0.45	186.3/121.3
S8(21/10)	9.53	9.51	14.46	9.36	8.91	8.45	57.49	58.27	-0.78	186.3/121.3
S9	8.9	8.79	13.37	8.79	8.10	7.91	55.13	51.82	3.31	365.7/235.7
S9(29/1)	8.9	8.78	13.37	8.73	8.10	7.91	55.32	52.48	2.83	365.7/235.7
S9(21/10)	8.9	8.78	13.37	8.70	8.10	7.91	55.31	52.90	2.41	365.7/235.7

4.4 Results and Discussions of the Hypothetical Flow Situations at Different Mass Flows

1) Table 3 confirms the observation m the previous Results section that when the mass flow decreases, an increase in heat loss per unit mass of fluid raises water level B. This is *caused* by the lower fluid velocities thus longer residence time in the pipelines. As a consequence AWL can decrease to a negative value. This also mean that Water Level B will drop as the mass flow increases but not lower than the calculated level when heat loss is assumed zero. The results also show that the assumption that water level B will remain stationary when mass flow changes is only true when pipe heat loss is assumed zero. Heat loss distorts this assumption.

Table 3. Pressures and water levels of hypothetical flow situations with increasing mass flow.

Situation	P1	P2	P3	P4	P5	P6
	(bars abs)	(bars abs)	(bars abs)	(bars abs)	(bars abs)	(bars abs)
S7a(21/10)-50	9.53	9.28	14.0958	9.13	8.71	8.39
S7(21/10)	9.53	9.28	14.1100	9.17	8.71	8.39
S7b(21/10)+50	9.53	9.28	14.1280	9.19	8.71	8.39
S7a(29/1)-50	9.53	9.30	14.0958	9.18	8.71	8.39
S7(29/1)	9.53	9.30	14.1100	9.20	8.71	8.39
S7b(29/1)+50	9.53	9.30	14.1280	9.22	8.71	8.39
Situation	**Water Level A**	**Water Level B**	**ΔWL**	**Mass Flow**	**Heat Loss**	
	(m)	(m)	(m)	(kg/s)	(m)	
S7a(21/10)-50	55.66	56.58	-0.92	159.6	311.13	
S7(21/10)	56.23	56.11	0.12	209.6	236.91	
S7b(21/10)+50	56.97	55.88	1.09	259.6	191.28	
S7a(29/1)-50	55.44	56.02	-0.58	159.6	249.99	
S7(29/1)	56.00	55.78	0.22	209.6	190.35	
S7b(29/1)+50	56.74	55.55	1.19	259.6	153.69	

2) The change in water levels due to the combined change in the mass flow and heat loss rate is relatively small due to their opposite effects. A more important finding is the occurrence of boiling 10 meters vertical distance below the hump on its upstream side. This might prove significant when pressure transient analysis is conducted on this model.

3) The above results show the need for very accurate measuring instruments to detect significant changes in pressure and thus prove some of the assumptions in this study.

5.0 CONCLUSIONS

1) Two-phase flow can occur as low as 10 meters vertical distance below the Hump Station in the ascending part of the pipeline after the RI System modification.

2) The single phase liquid column height between the Low Point and the Hump Station rises as the pipe heat loss increases due to the drop in saturation pressure of the fluid.

3) The water column free surface between the Separator Station and Low point backs up as the mass flow, pipe fiiction factor or heat loss increases.

4) The single-phase liquid column height between Low Point and the Hump Station rises as the mass flow decreases due to the drop in the saturation pressure of the fluid associated with the increase in heat loss per unit mass of fluid.

5) The single-phase liquid column height between Low Point and the Hump Station tends to be stationary as the pipe fiction factor increases.

6) The changes in the water levels of the Steady State Flow Model as the mass flow and heat loss change are not big enough to influence RI line utilization strategy.

6.0 RECOMMENDATIONS

Since the changes brought by mass flow and heat loss variations to the Steady State Flow Model are not that significant, the present operating procedure and Reinjection line utilization strategy need not to be modified until computerized pressure transient simulation proves otherwise.

7.0 NOMENCLATURE

A_n	Cross sectional area at point n, m^2
C	Heat conductance, W/m-K
D	Diameter, m
D_H	Hydraulic diameter, m
g	Acceleration due to gravity, m/sec^2
HS	Hump Station
HGL	Hydraulic Gradient Line
h	Specific Enthalpy, KJ/kg
h_f	Friction Loss, m
h_{f3-4}	Friction Loss between points 3 & 4, m
h_i	Internal heat transfer coefficient, KW/m^2-K
h_o	External heat transfer coefficient, KW/m^2-K
h_q	Heat loss of fluid, KJ/kg
h_{q3-4}	Heat loss of fluid between points 3 & 4, KJ/kg
k_{fg}	Thermal conductivity of fiber glass, W/m-K
k_p	Thermal conductivity of Perlite, W/m-K
k_s	Thermal conductivity of steel, W/m-K
λ	Friction factor
L	Length, m
LPS	Low Point Station
M	Mass flow, kg/s
P	Pressure, bar abs
$P_1, P_2 \ldots$	Pressure at point 1, point 2, bar abs

P1	Point 1, fixed on the 600-mm RI line immediately downstream of SSI where a pressure transmitter is located
P2	Point 2, moving point on the 600-mm RI line representing the water level between SS1 and LPS (water level A)
P3	Point 3, the lowest point on the 600-mm RI line located at the LPS where a pressure transmitter is also situated
P4	Point 4, moving point on the 600-mm RI line representing the water level between LPS & HS (water level B)
P5	Point 5, fixed on the 600-mm RI Line at the Hump where a pressure transmitter is also located
Q/L	Heat loss per unit length of pipeline, KJ/m
R_H	Hydraulic radius, m
ρ	Fluid Density, kg/m^3
s7, S8, s9	Flow situation 7,8 & 9 defined in the Methodology
S7(21/10)	Flow situation 7 with assumed ambient temperature of 21 deg C and wind speed of 10 m/s
S8(29/1)	Flow situation 8 with assumed ambient temperature of 29 deg C and wind speed of 1 m/s
S7a(21/10)-50	Flow situation based on S7 at a mass flow 50kg/s less, ambient temperature of 21 deg C and wind *speed* of 10 m/s
S7b(29/1)+50	Flow situation based on S7 at a mass flow 50kg/s more, ambient temperature of 29 deg C and wind speed of 1 m/s
SFEE	Steady Flow Energy Equation
SS1	Separator Station 1
ss2	Separator station 2
T	Temperature, deg C
AT	Difference in temperature, deg C
AWL.	Difference in Water level A & B, m
V	Fluid mean velocity, m/s
Z	Elevation of a point relative to the LPS, m

REFERENCES

Chaudry, M.H., 1979. Applied Hydraulic Transients. Litton Educational Publishing, Inc., New York, USA.

Daza, M.V., 1991. Pressure Transient Analysis. Project Report, Geothermal Institute, University of Auckland, New Zealand.

Kingston, Reynolds, Thoms and Allardice (KRTA) Consultants, 1988. Bacon Manito Geothermal Project, Review of Steam Gathering System Conceptual Design.

Llenarizas, L.J., 1992. Minimizing Pressure Transient Effects on Bacman 1 Reinjection System. Project Report, Geothermal Institute, University of Auckland, New Zealand

Obate, RD., 1989. Pipeline Hydraulic Transients. Project Report, Geothermal Institute, University of Auckland, New Zealand.

Perry R.H., and D.W. Green, 1984. Perry's Chemical Engineer's Handbook. McGraw-Hill Book Company Inc., 6th edition.

Rogers, G.F.C. and Y.R Mayhew, 1980. Engineering Thermodynamics. Longman Group Limited.

White, F.M., 1979. Fluid Mechanics. McGraw-Hill Kogakusha Limited.